Letters

A Magnetically Controlled *CLLC*-DCX Converter With Output Regulation Capability

Ting Luo, Quanming Luo, *Member, IEEE*, and Yuqi Wei, *Member, IEEE*

***Abstract*—The *CLLC* resonant converter operating in dc transformer (DCX) mode has excellent features, such as fixed switching frequency, load-independent voltage gain, full zero-voltage switching operation, and simple synchronous rectifier control, but the output voltage cannot be adjusted. To address this issue, this letter proposes a magnetically controlled *CLLC*-DCX converter based on variable resonant inductors. The proposed control method adjusts resonant inductors to change the equivalent transformer turns ratio n_e while keeping the resonant frequency fixed. Finally, an experimental prototype is built to validate the proposed magnetic control method.**

***Index Terms*—*CLLC* resonant converter, magnetic control, resonant power conversion.**

I. Introduction

THE *CLLC* converter, as shown in Fig. 1, is an ideal topology for isolated bidirectional dc–dc converter due to its high efficiency and wide zero-voltage switching (ZVS) operation range, which is often considered a bidirectional version of the *LLC* converter [1]. Similar to the *LLC* converter, pulse frequency modulation (PFM) is commonly utilized to regulate the output voltage [2], [3].

As shown in Fig. 2, the PFM adjusts the voltage gain by varying the switching frequency, in which the ac impedance of the resonant tank varies with frequency. For S-type *CLLC* ($L_pC_p = L_sC_s$) [2], if the switching frequency f_s equals the resonant frequency

$$f_r = \frac{1}{2\pi\sqrt{L_pC_p}} \tag{1}$$

then the ac impedance on both sides of transformer will be zero. Therefore, the normalized voltage gain $m = nV_2/V_1$ for resonant point operation ($f_n = f_s/f_r = 1$) is fixed at 1. This mode of operation, also known as dc transformer (DCX) mode, offers advantages, such as load-independent voltage gain, simple synchronous rectifier control, and full ZVS operation. The only drawback is that the output is not adjustable and usually requires an isolated auxiliary converter in series on the output side [4], [5].

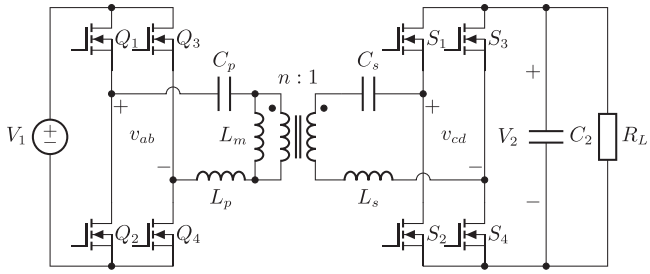

Fig. 1. Diagram of *CLLC* converter.

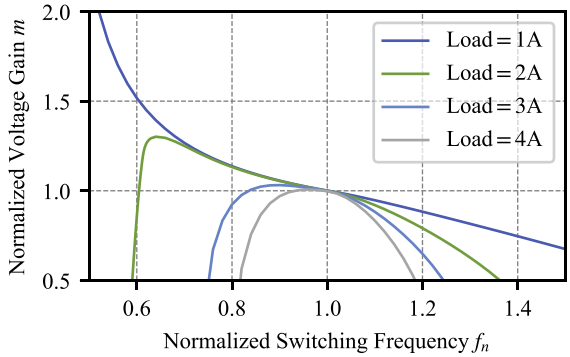

Fig. 2. Normalized voltage gain curve of *CLLC* converter at different load current with PFM control.

With PFM, as shown in Fig. 2, the regulation of the output voltage under light-load buck operation requires a significant change in frequency, while the voltage gain even decreases with frequency reduction under heavy-load boost operation. Moreover, a wide operating frequency range will cause some problems, such as unsatisfactory electromagnetic interference (EMI) performance and complicated design of magnetic components [6].

The structure of a current controlled variable inductor is shown in Fig. 3(a). The control winding is divided into two identical parts with the number of turns N_{DC}, and they are mounted on the left and right legs of the core, respectively. The

Received 4 July 2025; revised 15 August 2025; accepted 26 August 2025. Date of publication 3 September 2025; date of current version 22 October 2025. This work was supported by the National Natural Science Foundation of China under Grant U24B2097. *(Corresponding author: Quanming Luo.)*

Ting Luo and Quanming Luo are with the School of Electrical Engineering, Chongqing University, Chongqing 400044, China (e-mail: 20123958@cqu.edu.cn; lgm394@cqu.edu.cn).

Yuqi Wei is with the School of Electrical Engineering, Xi'an Jiaotong University, Xi'an 710049, China (e-mail: yuqiwei@xjtu.edu.cn).

Digital Object Identifier 10.1109/TPEL.2025.3605885

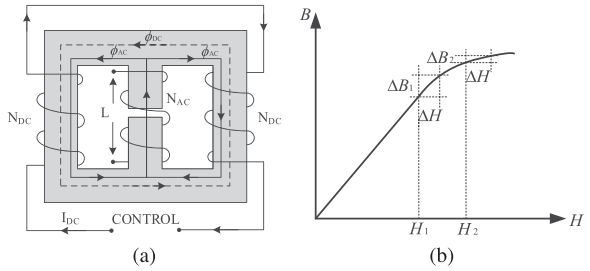

Fig. 3. Current controlled variable inductor. (a) Structure. (b) Principle of operation.

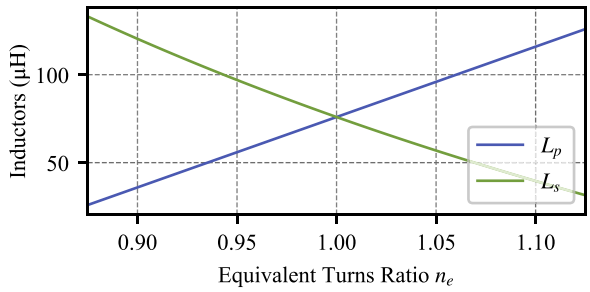

Fig. 5. Resonant inductors vary with equivalent turns ratio n_e.

TABLE I
DESIGN SPECIFICATIONS

Parameter	Symbol	Value
Input voltage	V_1	200V
Output voltage	V_2	180–225V
Switching frequency	f_s	100kHz
Resonant frequency	f_r	100kHz
Transformer magnetizing inductor	L_m	400μH
Variable inductance range	$L_{\max}/L_{\min}$	4

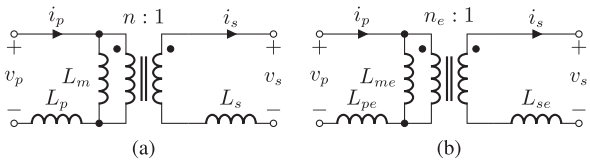

Fig. 4. Magnetic part of *CLLC* converter. (a) Original. (b) Equivalent.

TABLE II
MAIN PARAMETERS OF THE *CLLC* CONVERTER

Parameter	Value
Transformer	Material: PC95, bobbin: PQ5050 $L_m = 400\mu$H, $n = 1$ N_1-24 turns of litz wire (ϕ 0.1mm * 100) N_2-24 turns of litz wire (ϕ 0.1mm * 100)
Inductors	Material: PC44, bobbin: PQ4040 $L_{p_\max} = L_{s_\max} = 128\mu$H $L_{p_\min} = L_{s_\min} = 32\mu$H N_{AC}-8 turns of litz wire (ϕ 0.1mm * 100) N_{DC}-20 turns of litz wire (ϕ 0.1mm * 25)
Capacitors	Metallized polypropylene film capacitors (MKP) $C_p = C_s = 33$nF, $C_2 = 35\mu$F
Switches	SCT3060AL (ROHM), $R_{DS(on)} = 80$mΩ $C_{oss} = 100$pF, $f_s = 100$kHz, $t_{dead} = 100$ns

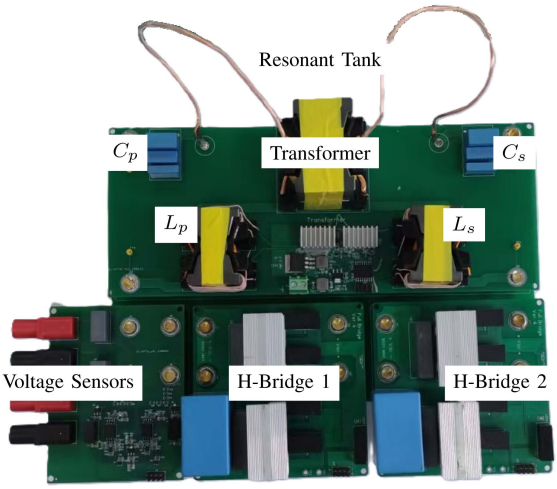

Fig. 6. Experimental prototype.

inductor winding, with the number of turns N_{AC}, is placed on the air-gapped middle leg of the core. The control current generates a dc bias magnetic flux density inside the magnetic core, thus the material magnetic permeability is adjusted by changing the dc operating point around the knee of the B–H curve, as shown in Fig. 3(b). There are also other improved types of variable inductors suitable for various application scenarios [7], [8].

By utilizing variable inductor as resonant inductor, f_r will be adjustable so that f_n can be regulated and thus the output voltage with fixed f_s . This type of strategies has been applied to *LLC* converters [6], [9]. Similar strategies can certainly be migrated to *CLLC* converters, but this letter presents an alternative magnetically control method.

This proposed method regulates the output voltage by varying the equivalent transformer turns ratio n_e instead of the voltage gain m. Adjusting the resonant inductors based on the parameter equivalent ensures that the resonant frequency remains constant, and n_e can be freely adjusted. Compared with previous control strategies, it allows the *CLLC* converter to maintain the DCX mode at different V_2/V_1.

The rest of this letter is organized as follows. Section II provides the derivation of parameter equivalent principle. In Section III, the parameter design method of magnetically controlled *CLLC* is introduced. Experimental results are provided in Section IV. Finally, Section V concludes this letter.

II. PARAMETER EQUIVALENT

The magnetic network of the *CLLC* converter, as shown in Fig. 4(a), comprises three inductances (L_p, L_s, and L_m) and an ideal transformer characterized by its turns ratio n. Since these three inductors are not fully independent, there exists an alternative set of circuit parameters (L_{pe}, L_{se}, L_{me}, and n_e), as shown in Fig. 4(b), that yields identical external electrical characteristics.

If the circuits in Fig. 4(a) and (b) exhibit identical external characteristics, then the following relationship holds:

$$\begin{bmatrix} v_p \\ v_s \end{bmatrix} = \begin{bmatrix} L_p + L_m & \frac{L_m}{n} \\ \frac{L_m}{n} & L_s + \frac{L_m}{n^2} \end{bmatrix} \begin{bmatrix} \frac{di_p}{dt} \\ \frac{-di_s}{dt} \end{bmatrix} \tag{2}$$

and

$$\begin{bmatrix} L_p + L_m & \frac{L_m}{n} \\ \frac{L_m}{n} & L_s + \frac{L_m}{n^2} \end{bmatrix} = \begin{bmatrix} L_{pe} + L_{me} & \frac{L_{me}}{n_e} \\ \frac{L_{me}}{n_e} & L_{se} + \frac{L_{me}}{n_e^2} \end{bmatrix}. \tag{3}$$

Since the diagonal elements are identical, (3) provides only three independent equations but four unknown parameters. This allows the introduction of an additional constraint. For S-type equivalent circuit, one may assign $L_{pe}C_p = L_{se}C_s$, then the equivalent circuit parameters are given by

$$\begin{cases} n_e &= \left(\sqrt{b^2 + 4/h} - b\right)/2 \\ L_{me} &= n_e L_m / n \\ L_{pe} &= L_p + L_m - L_{me} \\ L_{se} &= L_s + L_m/n^2 - L_{me}/n_e^2 \end{cases} \tag{4}$$

where

$$b = n\left(\frac{L_s}{hL_m} - \frac{L_p}{L_m} - 1\right) + \frac{1}{hn} \tag{5}$$

$$h = C_p/C_s. \tag{6}$$

III. Parameter Design

With the design specifications in Table I as an example, this section presents the circuit parameters design methodology for a magnetically controlled symmetric *CLLC*-DCX converter. The value of $L_{\max}/L_{\min}$ is directly provided in Table I, as it can be approximately estimated based on the core material and the maximum dc magnetic field strength.

First, based on the symmetry

$$\begin{cases} L_{pe} &= n^2 L_{se} \\ C_s &= n^2 C_p. \end{cases} \tag{7}$$

For the S-type equivalent circuit, it is necessary that L_{pe} and L_{se} are constant to keep the resonant frequency f_r fixed. For different n_e, values of L_p and L_s can be obtained according to (4) as follows:

$$\begin{cases} L_p &= L_{pe} + n_e L_m/n - L_m \\ n^2 L_s &= n^2 L_{se} + nL_m/n_e - L_m \end{cases} \tag{8}$$

where L_{pe}, L_{se}, and n are unknown constants to be calculated. Since m is fixed at 1, the output can be regulated as follows:

$$V_2 = V_1/n_e. \tag{9}$$

Then, the range of equivalent turns ratio n_e should be

$$n_{e\_\max} = V_{1\_\max}/V_{2\_\min} = 1.125 \tag{10}$$

$$n_{e\_\min} = V_{1\_\min}/V_{2\_\max} = 0.9 \tag{11}$$

where, in this example, $V_{1\_\max} = V_{1\_\min} = V_1$.

To ensure that L_p and $n^2 L_s$ have the same range of variation, from (8), there is

$$n = \sqrt{n_{e\_\min} n_{e\_\max}} = 1 \tag{12}$$

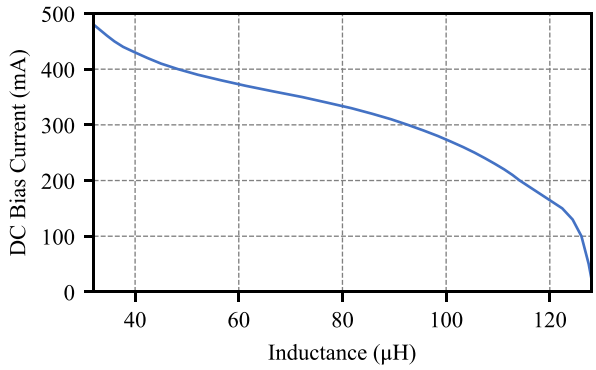

Fig. 7. Relationship between DC bias current and variable inductance value.

and

$$L_{p\_\max} - L_{p\_\min} = (n_{e\_\max} - n_{e\_\min})\frac{L_m}{n} = 90\mu\text{H}. \tag{13}$$

Since $L_{\max}/L_{\min} = 4$, there are

$$\begin{cases} L_{p\_\max} &= n^2 L_{s\_\max} = 120\mu\text{H} \\ L_{p\_\min} &= n^2 L_{s\_\min} = 30\mu\text{H} \end{cases} \tag{14}$$

and

$$L_{pe} = n^2 L_{se} = L_{p\_\max} - \frac{n_{e\_\max}}{n} L_m + L_m = 70\mu\text{H}. \tag{15}$$

Then, the variations of L_p and L_s with n_e for the example of Table I are shown in Fig. 5. The resonant capacitors are selected as follows:

$$C_p = \frac{C_s}{n^2} = \frac{1}{L_{pe}(2\pi f_r)^2} = 36\text{nF}. \tag{16}$$

IV. Experiment

To verify the proposed control method, an experimental prototype with parameters in Table II was built, as shown in Fig. 6. The relationship between the inductance of the designed variable inductor and its dc bias current is shown in Fig. 7. The inductance decreases from 128 to 32 μH when the dc bias current increases from 0 to 0.48 A, which satisfies the system requirement.

The closed-loop control block diagram of the proposed method is shown in Fig. 8, where the proportional-integral (PI) regulator adjusts the output voltage by varying n_e. The inductances of the variable inductors L_p and L_s are calculated from (8), and then the output currents of the controlled current sources are obtained from the inductance–current (*L–I*) curve shown in Fig. 7. The control circuit of the variable inductor is shown in Fig. 9. The output of *L–I* curve in Fig. 8 is transmitted to the digital-to-analog converter (DAC) via serial peripheral interface (SPI), converted into a voltage signal, and then delivered to the voltage-controlled current source consisting of an operational amplifier and an negative-positive-negative (NPN) bipolar junction transistor.

Fig. 10 presents the transient waveforms under input voltage variations, showing that the output voltage remains consistent before and after the change, thereby demonstrating that the proposed method achieves closed-loop control.

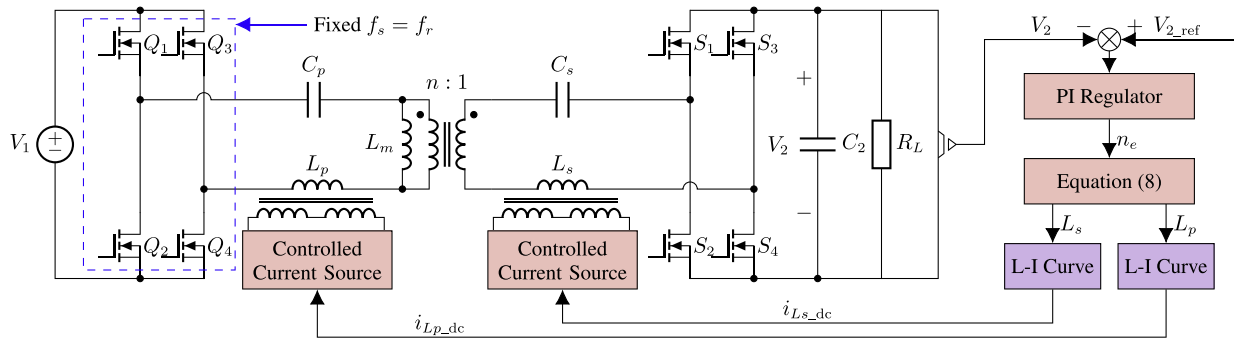

Fig. 8. Control diagram of the proposed magnetically-controlled *CLLC*-DCX converter.

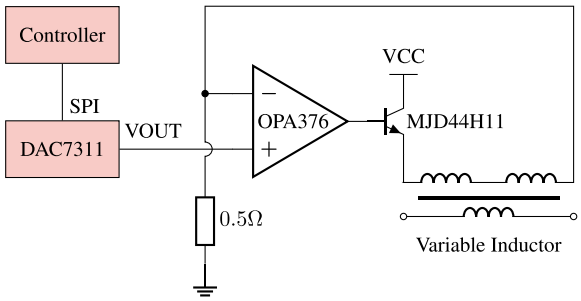

Fig. 9. Control circuit of the variable inductor.

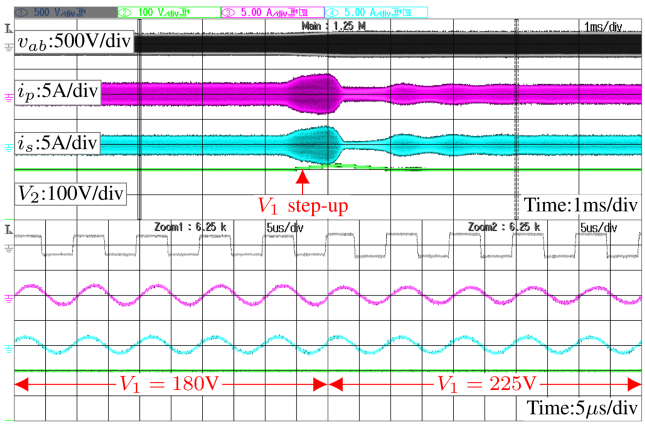

Fig. 10. Step response with zoomed views of V_1 changes from 180 to 225 V when $V_{2\_\mathrm{ref}} = 200$ V and $R_L = 200\Omega$.

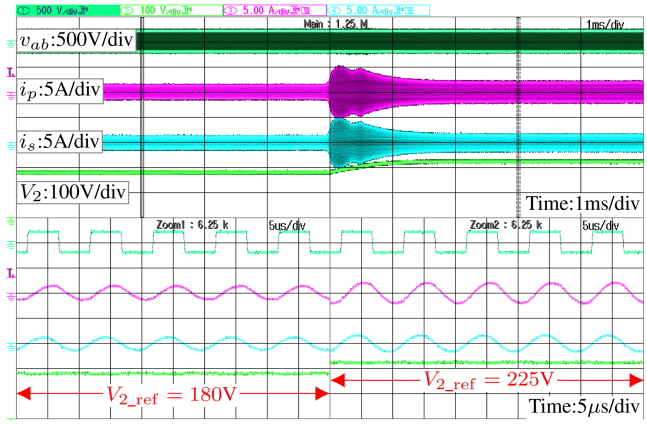

Fig. 11. Step response with zoomed views of V_{2_ref} changes from 180 to 225 V when $V_1 = 200$ V and $R_L = 200\Omega$.

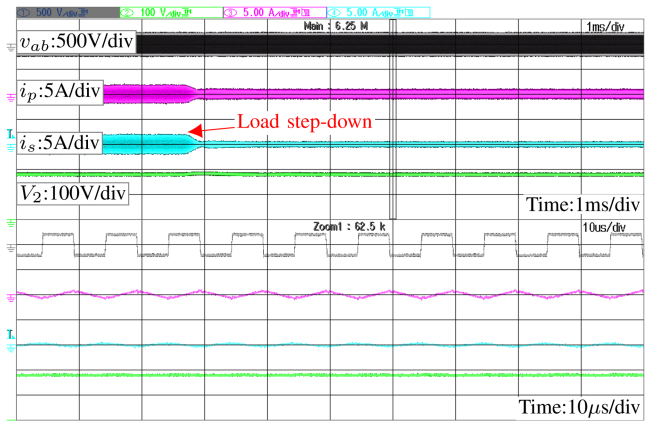

Fig. 12. Step response with zoomed view of R_L changes from 162 Ω to ∞ when $V_1 = 200$ V and $V_{2\_\mathrm{ref}} = 180$ V.

The step response waveforms of the prototype when $V_1 = 200$ V and reference output voltage V_{2_ref} changes from 180 to 225 V are shown in Fig. 11. In both Figs. 10 and 11, the switching frequency remains fixed before and after the voltage steps, and the waveforms of the resonant currents are approximately sinusoidal. This indicates that the proposed control method can achieve the DCX mode at different V_1/V_2.

As shown in Fig. 12, the proposed magnetic control converter can maintain the output voltage at its minimum value when the load changes from full load to no load.

Fig. 13 presents a comparative analysis of dynamic responses with same PI parameters. As illustrated in Fig. 13(a), the PFM control scheme (with fixed $L_p = L_s = 77$ μH) exhibits a significant switching frequency variation from 179.2 to 119.6 kHz during the load transient. In contrast, Fig. 13(b) demonstrates that the proposed magnetic control method maintains greater

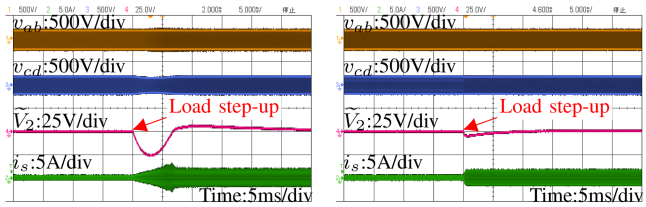

Fig. 13. Dynamic response when load steps from 50 to 200 W at $V_1 = 200$ V and $V_{2\_ref} = 180$ V. (a) PFM control. (b) Proposed magnetic control.

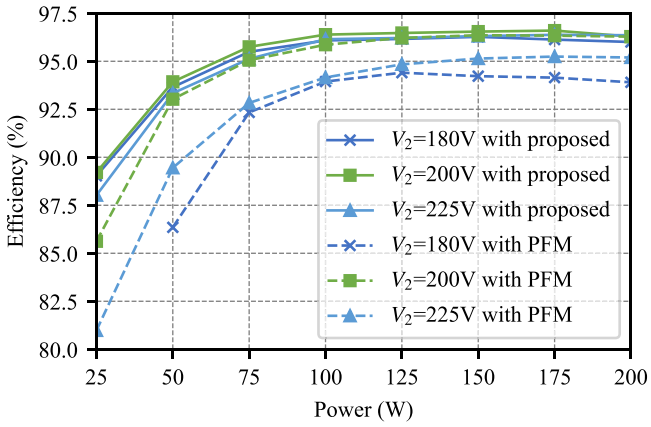

Fig. 14. Measured efficiency at different output when $V_1 = 200$ V.

stability, with the n_e showing only a minor adjustment from 1.098 to 1.074.

The efficiency curves at different output are shown in Fig. 14, where the efficiency varies little over the entire voltage gain range. The highest efficiency with 200 W load is 96.3% at $V_2 = 200$ V and the lowest is 96% at $V_2 = 180$ V. For PFM control with synchronous rectification, the efficiency curve at $V_2 = 180$ V is incomplete since the voltage gain cannot be satisfied at light load.

Both control methods exhibit an efficiency drop under light-load conditions, mainly because the transformer magnetizing current does not decrease significantly at light load, and the proportion of losses caused by it increases as the total power decreases. Compared with PFM control, the proposed magnetic control method can improve efficiency over the entire power range, especially when m deviates from 1.

V. Conclusion

In this letter, a magnetically controlled *CLLC* converter is proposed. Compared with previous converters, it varies the equivalent transformer turns ratio n_e instead of voltage gain m to regulate the output. Thus, the converter can operate in DCX mode with fixed $m = 1$ at different V_1/V_2, which brings the benefits of fixed switching frequency, simple synchronous rectification control, load independent voltage gain, and full ZVS operation. Finally, the proposed closed-loop control and parameter design methods are experimentally validated.

References

[1] R. Yu, G. K. Y. Ho, B. M. H. Pong, B. W.-K. Ling, and J. Lam, "Computer-aided design and optimization of high-efficiency LLC series resonant converter," *IEEE Trans. Power Electron.*, vol. 27, no. 7, pp. 3243–3256, Jul. 2012.

[2] L. Zhao, Y. Pei, L. Wang, L. Pei, W. Cao, and Y. Gan, "Design methodology of bidirectional resonant CLLC charger for wide voltage range based on parameter equivalent and time domain model," *IEEE Trans. Power Electron.*, vol. 37, no. 10, pp. 12041–12064, Oct. 2022.

[3] T. Luo et al., "A full-iteration optimal design methodology of CLLC converter with minimized RMS current," *IEEE Trans. Power Electron.*, vol. 39, no. 10, pp. 11916–11930, Oct. 2024.

[4] W. Feng, P. Mattavelli, and F. C. Lee, "Pulsewidth locked loop (PWLL) for automatic resonant frequency tracking in LLC DC–DC transformer (LLC -DCX)," *IEEE Trans. Power Electron.*, vol. 28, no. 4, pp. 1862–1869, Apr. 2013.

[5] X. Wu, H. Chen, and Z. Qian, "1-MHz LLC resonant DC transformer (DCX) with regulating capability," *IEEE Trans. Ind. Electron.*, vol. 63, no. 5, pp. 2904–2912, May 2016.

[6] Y. Wei, Q. Luo, X. Du, N. Altin, J. M. Alonso, and H. A. Mantooth, "Analysis and design of the LLC resonant converter with variable inductor control based on time-domain analysis," *IEEE Trans. Ind. Electron.*, vol. 67, no. 7, pp. 5432–5443, Jul. 2020.

[7] D. T. Isaac and J.-H. Park, "Performance enhancement of multi-resonant high-Q converters using a variable resonator element," in *Proc. 7th Int. Conf. Power Electron. Syst. Appl. - Smart Mobility, Power Transfer & Secur.*, , 2017,, pp. 1–6.

[8] Y. Lu, Y. Yang, and L. Zhang, "Design of LLC resonant converter based on magnetic-valve variable resonant inductor for wide input voltage range," in *Proc. CPSS IEEE Int. Symp. Energy Storage Convers.*, 2024, pp. 1050–1055.

[9] J. M. Alonso, M. S. Perdigão, D. G. Vaquero, A. J. Calleja, and E. S. Saraiva, "Analysis, design, and experimentation on constant-frequency DC-DC resonant converters with magnetic control," *IEEE Trans. Power Electron.*, vol. 27, no. 3, pp. 1369–1382, Mar. 2012.